

Nitrogen loss from soil through anaerobic ammonium oxidation coupled to iron reduction

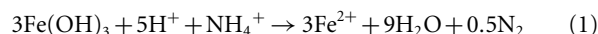
Wendy H. Yang^{1*}, Karrie A. Weber² and Whendee L. Silver¹

The oxidation of ammonium is a key step in the nitrogen cycle, regulating the production of nitrate, nitrous oxide and dinitrogen. In marine and freshwater ecosystems, anaerobic ammonium oxidation coupled to nitrite reduction, termed anammox, accounts for up to 67% of dinitrogen production^{1–3}. Dinitrogen production through anaerobic ammonium oxidation has not been observed in terrestrial ecosystems, but the anaerobic oxidation of ammonium to nitrite has been observed in wetland soils under iron-reducing conditions^{4,5}. Here, we incubate tropical upland soil slurries with isotopically labelled ammonium and iron(III) to assess the potential for anaerobic ammonium oxidation coupled to iron(III) reduction, otherwise known as Feammox⁶, in these soils. We show that Feammox can produce dinitrogen, nitrite or nitrate in tropical upland soils. Direct dinitrogen production was the dominant Feammox pathway, short-circuiting the nitrogen cycle and resulting in ecosystem nitrogen losses. Rates were comparable to aerobic nitrification^{7,8} and to denitrification⁹, the latter being the only other process known to produce dinitrogen in terrestrial ecosystems. We suggest that Feammox could fuel nitrogen losses in ecosystems rich in poorly crystalline iron minerals, with low or fluctuating redox conditions.

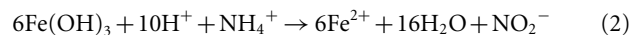
Terrestrial net primary productivity is often limited by the availability of fixed nitrogen (N) owing in large part to the mobility of N across ecosystem boundaries, particularly through denitrification¹⁰. Denitrification is dominantly a microbial process that converts nitrate (NO₃⁻) to nitrous oxide (N₂O) and dinitrogen (N₂) gases. In terrestrial ecosystems, denitrification is thought to be the only process by which fixed N is converted to N₂, thereby completing the nitrogen cycle. In aquatic systems, anammox bypasses the potential for N₂O production as well as decreasing internal N cycling. Bacteria capable of anammox have been detected in soil^{11,12}, but the occurrence of anammox has not been demonstrated in terrestrial ecosystems¹³.

The reduction of ferric iron (Fe(III)) can be coupled to anaerobic ammonium (NH₄⁺) oxidation to produce N₂ (ref. 14), NO₃⁻ (ref. 14), or NO₂⁻ (refs 4–6). This process is termed Feammox⁶ and theoretically could occur abiotically or be microbially mediated. There is some evidence of Feammox to NO₂⁻ in wetland soils^{4,5}, but Feammox to N₂ has not been previously described nor has Feammox been measured in upland soils. Feammox to N₂ is energetically more favourable than Feammox to NO₂⁻ or NO₃⁻ and is favourable over a wider range of conditions. Environments rich in poorly crystalline Fe minerals, such as highly weathered soils, have the potential to support Feammox. Under conditions typically found in soil, Feammox to N₂ using ferrihydrite, a common poorly crystalline Fe oxide, yields

–245 kJ mol⁻¹ reaction (see Supplementary Equations) through the following process (equation (1)):



This reaction remains energetically favourable over a wide pH range. Feammox to NO₂⁻ (equation (2)) occurs only below pH 6.5, stoichiometrically requires more Fe(III) and yields less energy than Feammox to N₂ (–164 kJ mol⁻¹ reaction) under the same conditions:



Feammox to NO₃⁻ is also thermodynamically feasible under these conditions (–207 kJ mol⁻¹ reaction).

Feammox rates averaged 1.20 ± 0.28 μg N g⁻¹ d⁻¹ (±standard error of the mean) following the addition of both ¹⁵NH₄⁺ and Fe(III) to a tropical forest soil (Fig. 1a). These rates are conservative estimates determined from ³⁰N₂ production alone and are comparable to gross aerobic nitrification rates in tropical forests^{7,8,15}. Lower ³⁰N₂ production occurred following the addition of ¹⁵NH₄⁺ alone (0.32 ± 0.13 μg N g⁻¹ d⁻¹, *p* < 0.001), presumably resulting from the utilization of background Fe in the Feammox reaction. These soils are rich in poorly crystalline, reactive Fe (6.2 ± 0.2 mg Fe g⁻¹ soil¹⁶); thus, sufficient background Fe(III) was available to drive ³⁰N₂ production with the addition of ¹⁵NH₄⁺ alone. At 24 h after ¹⁵NH₄⁺ addition, HCl-extractable Fe(III) concentrations averaged 528 ± 128 μg Fe(III) g⁻¹. We used replicate (*n* = 8) upland soils (0–10 cm depth) from the Luquillo Mountains, Puerto Rico, USA. Soils were slurried and pre-incubated in an anaerobic glove box to remove O₂, inhibit aerobic nitrification and deplete background NO₂⁻ and NO₃⁻. Rigorous procedures were used to exclude molecular O₂ from the experiment thereby removing the possibility of aerobic nitrification (see Supplementary Discussion). We then measured ³⁰N₂ (³⁰N₂ = ¹⁵N + ¹⁵N) and ²⁹N₂ (²⁹N₂ = ¹⁵N + ¹⁴N) mole fractions of headspace gas in samples and soil-free jars (that is, blanks) to determine ³⁰N₂ and ²⁹N₂ production rates (see Supplementary Methods). Feammox directly to N₂ or Feammox-generated NO₂⁻ followed by denitrification or anammox are the only possible sources of ³⁰N₂ (Table 1). At least two possible mechanisms exist for Feammox: surface Fe reduction coupled to NH₄⁺ oxidation, or O₂ liberated from Fe oxides used for intra-aerobic NH₄⁺ oxidation coupled to Fe reduction, similar to anaerobic methane oxidation coupled to NO₂⁻ reduction carried out by oxygenic bacteria¹⁷.

¹Department of Environmental Science, Policy, and Management, University of California, Berkeley, California 94720, USA, ²School of Biological Sciences and Department of Earth and Atmospheric Sciences, University of Nebraska-Lincoln, Lincoln, Nebraska 68588, USA. *e-mail: wendy_yang@berkeley.edu.

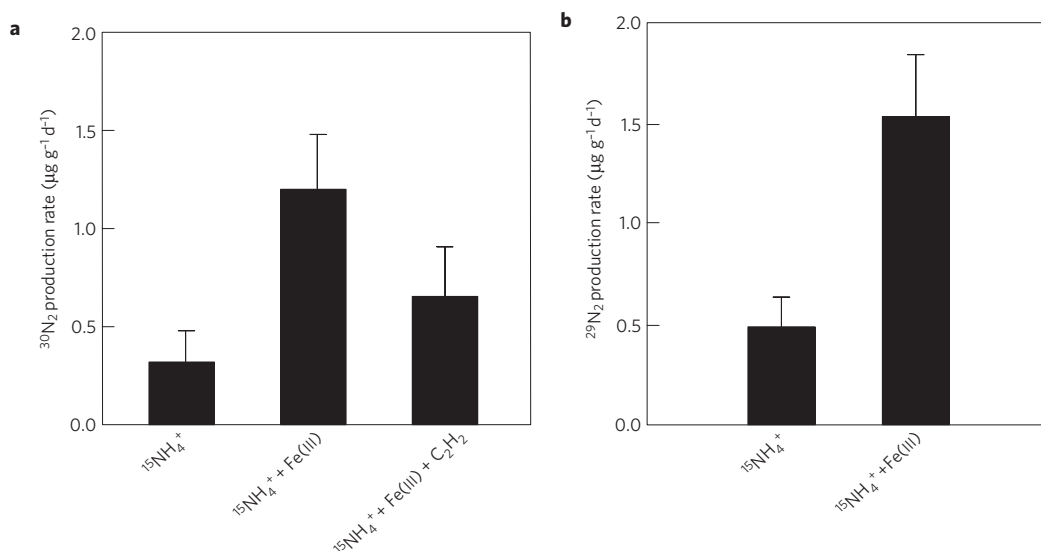


Figure 1 | Mean $^{30}\text{N}_2$ and $^{29}\text{N}_2$ production rates. a, Mean $^{30}\text{N}_2$ production rates following the addition of $^{15}\text{NH}_4^+$, $^{15}\text{NH}_4^+ + \text{Fe(III)}$ or $^{15}\text{NH}_4^+ + \text{Fe(III)} + \text{C}_2\text{H}_2$. The addition of Fe(III) and Fe(III) + C_2H_2 significantly increased mass $^{30}\text{N}_2$ relative to $^{15}\text{NH}_4^+$ alone ($p < 0.001$, $p = 0.08$, respectively). **b,** Mean $^{29}\text{N}_2$ production rates following the addition of $^{15}\text{NH}_4^+$ or $^{15}\text{NH}_4^+ + \text{Fe(III)}$ ($p = 0.02$). Error bars represent standard errors ($n = 8$).

Table 1 | Potential pathways for $^{30}\text{N}_2$ and $^{29}\text{N}_2$ production from $^{15}\text{NH}_4^+$ under anoxic conditions.*

Product	Nitrogen substrate 1	Nitrogen substrate 2	Process
$^{30}\text{N}_2$	Added $^{15}\text{NH}_4^+$	Added $^{15}\text{NH}_4^+$	Feammox to N_2
	Added $^{15}\text{NH}_4^+$	Feammox-generated $^{15}\text{NO}_2^- / ^{15}\text{NO}_3^-$	Anammox
	Feammox-generated $^{15}\text{NO}_2^- / ^{15}\text{NO}_3^-$	Feammox-generated $^{15}\text{NO}_2^- / ^{15}\text{NO}_3^-$	Denitrification
$^{29}\text{N}_2$	Added $^{15}\text{NH}_4^+$	Background $^{14}\text{NH}_4^+$	Feammox to N_2
	Added $^{15}\text{NH}_4^+$	Background $^{14}\text{NO}_2^- / ^{14}\text{NO}_3^-$	Anammox
	Feammox-generated $^{15}\text{NO}_2^- / ^{15}\text{NO}_3^-$	Background $^{14}\text{NH}_4^+$	Anammox
	Feammox-generated $^{15}\text{NO}_2^- / ^{15}\text{NO}_3^-$	Background $^{14}\text{NO}_2^- / ^{14}\text{NO}_3^-$	Denitrification
	Feammox-generated $^{15}\text{NO}_2^- / ^{15}\text{NO}_3^-$	Background $^{14}\text{NO}_2^- / ^{14}\text{NO}_3^-$	Denitrification

*Dissimilatory NO_3^- reduction to NH_4^+ cycles background $^{14}\text{NO}_2^- / ^{14}\text{NO}_3^-$ or Feammox-generated $^{15}\text{NO}_2^- / ^{15}\text{NO}_3^-$ to $^{14}\text{NH}_4^+$ or $^{15}\text{NH}_4^+$, respectively. Thus, it does not create additional pathways for $^{30}\text{N}_2$ and $^{29}\text{N}_2$ production from $^{15}\text{NH}_4^+$. †Feammox can generate $^{15}\text{NO}_2^-$ or $^{15}\text{NO}_3^-$ from added $^{15}\text{NH}_4^+$.

Feammox directly to N_2 accounted for 47 (± 27) to 72 (± 9)% of $^{30}\text{N}_2$ loss in the Fe(III) and $^{15}\text{NH}_4^+$ treatment (see Supplementary Methods). We used acetylene (C_2H_2) to separate direct N_2 production through Feammox from gaseous N loss through denitrification of Feammox-generated NO_2^- and NO_3^- . Acetylene blocks the reduction of N_2O to N_2 (ref. 18), allowing N_2O produced from denitrification to accumulate in the headspace. The presence of C_2H_2 decreased $^{30}\text{N}_2$ production ($p = 0.08$; Fig. 1a), indicating that $53 \pm 27\%$ of $^{30}\text{N}_2$ loss resulted from Feammox to NO_2^- or NO_3^- . The rate of Feammox to NO_2^- or NO_3^- estimated from the difference in $^{30}\text{N}_2$ production with and without C_2H_2 addition was $0.59 \pm 0.32 \mu\text{g N g}^{-1} \text{d}^{-1}$. Based on N_2O production rates in the presence of C_2H_2 , approximately $0.33 \pm 0.08 \mu\text{g N g}^{-1} \text{d}^{-1}$ was oxidized to NO_2^- or NO_3^- and then subsequently reduced to N_2O through denitrification ($28 \pm 9\%$ of $^{30}\text{N}_2$ production). These two separate estimates suggest that Feammox directly to N_2 dominates as the gaseous N loss pathway.

We also measured significant $^{29}\text{N}_2$ production following the addition of $^{15}\text{NH}_4^+$ alone ($p = 0.03$) and following the addition of Fe(III) and $^{15}\text{NH}_4^+$ together ($p < 0.001$; Fig. 1b). The production rate of $^{29}\text{N}_2$ was significantly greater following Fe(III) and $^{15}\text{NH}_4^+$ addition compared with $^{15}\text{NH}_4^+$ addition alone ($p = 0.02$). Overall, $^{29}\text{N}_2$ accounted for $60 \pm 12\%$ of the total $^{15}\text{N}-\text{N}_2$ produced, which is consistent with the value of 66% predicted from random combinations of background $^{14}\text{NH}_4^+$ and added $^{15}\text{NH}_4^+$. The production of $^{29}\text{N}_2$ is interesting for several reasons. First,

the proportion of $^{29}\text{N}_2$ produced suggests that there was not preferential utilization of added $^{15}\text{NH}_4^+$ for N_2 production during the experiment, indicating that the $^{14}\text{NH}_4^+$ and $^{15}\text{NH}_4^+$ pools were well mixed. Second, there are several potential sources of $^{29}\text{N}_2$ including Feammox to NO_2^- followed by anammox to N_2 , the use of background $^{14}\text{NH}_4^+$ along with added $^{15}\text{NH}_4^+$ in Feammox to N_2 , or a combination of pathways involving Feammox-generated NO_2^- or NO_3^- followed by denitrification (Table 1). All of these pathways, however, require anaerobic NH_4^+ oxidation. Third, the stimulation of $^{29}\text{N}_2$ with Fe(III) addition further indicates that Feammox played an important role in anaerobic NH_4^+ oxidation, regardless of the ultimate mechanism for $^{29}\text{N}_2$ generation. Considering the production of both $^{30}\text{N}_2$ and $^{29}\text{N}_2$, anaerobic NH_4^+ oxidation consumed 5–14% of the added $^{15}\text{NH}_4^+$ label during the experiment.

In a time-series experiment $^{30}\text{N}_2$ production occurred rapidly, within 1.5 h of adding $^{15}\text{NH}_4^+$ and Fe(III) (Fig. 2). The change in $^{30}\text{N}_2$ mole fraction over 1.5 h was equivalent to Feammox rates of $0.48 \pm 0.11 \mu\text{g N g}^{-1} \text{d}^{-1}$. Feammox rates were relatively constant over 9 h and averaged $0.11 \pm 0.01 \mu\text{g N g}^{-1} \text{d}^{-1}$. These rates were lower than in the previous experiment, probably owing to the higher pH of the soil ($\text{pH } 5.21 \pm 0.28$ relative to 4.27 ± 0.02). Theoretically Feammox rates will decrease as pH increases because the reaction becomes less thermodynamically favourable and the reactivity of Fe oxide minerals decreases as pH increases¹⁹. To test this we conducted a third experiment in tropical forest soils with an initial

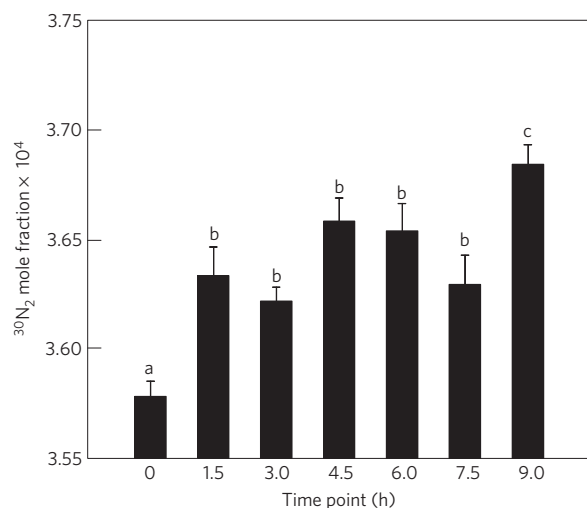


Figure 2 | Change in mean $^{30}\text{N}_2$ mole fraction over 9 h. Mean $^{30}\text{N}_2$ mole fraction following the addition of $^{15}\text{NH}_4^+$ + Fe(III) in the time-series experiment. Lowercase letters indicate statistically significant differences among time points using a repeated measures analysis of variance ($p < 0.05$). Bars are mean values ($n = 8$) and standard errors.

pH of 6.12 ± 0.03 . The rate of $^{30}\text{N}_2$ production following $^{15}\text{NH}_4^+$ and Fe(III) addition was considerably lower than under more acidic conditions ($0.02 \pm 0.01 \mu\text{g N g}^{-1} \text{d}^{-1}$ during the first 6 h) and did not vary significantly at 12 or 25 h (Fig. 3). Iron reduction increased by $115 \pm 67 \mu\text{g Fe(III) g}^{-1} \text{d}^{-1}$ with NH_4^+ and Fe(III) addition compared with NH_4^+ addition alone, approximately reflecting the $140 \mu\text{g Fe g}^{-1}$ of Fe(III) added. This suggests that the added Fe(III) was readily reducible, although only a small proportion of the Fe(III) reduced was likely to be associated with NH_4^+ oxidation (see Supplementary Methods).

In a series of calculations, we estimate a potential Feammox rate of $1\text{--}4 \text{ kg NH}_4^+\text{--N ha}^{-1} \text{y}^{-1}$ (0–10 cm depth). Incubations with added substrate may have stimulated Feammox under laboratory conditions and thus we used the theoretical ratios of 3–6 moles of Fe(III) reduced per mole of NH_4^+ oxidized based on the thermodynamic calculations instead of measured laboratory rates. Using this approach, only 0.4–0.8% of Fe reduction is attributable to Feammox. We assumed a mean Fe reduction rate of $25 \mu\text{g Fe g}^{-1} \text{d}^{-1}$ after weighting Fe reduction by the temporal O_2 dynamics previously measured at the field site²⁰. This rate of Fe reduction is considerably lower than those measured in the anaerobic slurries, which may have also been stimulated under laboratory conditions (see Supplementary Methods). These results suggest that Feammox is roughly equivalent to total denitrification estimated for this forest⁹. Similar to denitrification and aerobic nitrification, Feammox is likely to be highly variable in space and time owing to spatial and temporal heterogeneity in substrate availability, redox potential and pH.

Feammox provides alternative loss pathways of N from soils, decreasing N_2O emissions if NH_4^+ is oxidized directly to N_2 , or potentially increasing N_2O emissions if Feammox results in NO_2^- or NO_3^- followed by incomplete denitrification. However, here we indicate that Feammox to N_2 is the dominant gaseous N loss pathway. Our estimates here have considered Feammox only in the top 10 cm of soil, but NH_4^+ , Fe(III) and reducing conditions also occur deeper in the soil profile, increasing the importance of this NH_4^+ oxidation pathway. Feammox is likely to occur in Fe-rich soils that experience periods of anoxia or contain anoxic microsites. Frequent low-redox events have been measured in upland soils in humid regions, during periods of rainfall, or when O_2 consumption exceeds diffusive resupply^{20–24}.

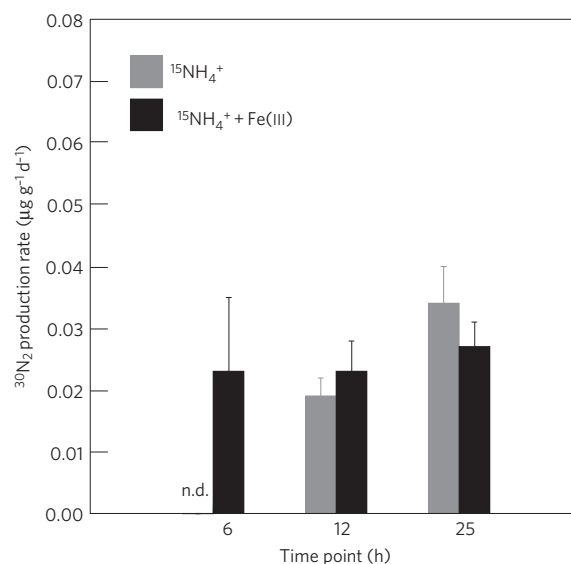


Figure 3 | Mean $^{30}\text{N}_2$ production rate at pH 6. Mean $^{30}\text{N}_2$ production rates following the addition of $^{15}\text{NH}_4^+$ or $^{15}\text{NH}_4^+$ + Fe(III) to tropical forest soils above pH 6. Error bars represent standard errors ($n = 8$). n.d. = not detectable within a detection limit of $0.007 \mu\text{g } ^{15}\text{N g}^{-1} \text{d}^{-1}$. There was no statistically significant increase in $^{30}\text{N}_2$ production with Fe(III) addition.

Even in well-drained soils, high rates of Fe reduction can occur in well-aggregated clay and organic colloids²⁵. Feammox has not been considered in ecosystem or global models of N cycling and could change our estimates of total N losses from terrestrial environments.

Methods

We slurried surface soil (0–10 cm depth) from the Luquillo Experimental Forest. Fresh soil was collected for each experiment on different dates at different locations and was transported to the University of California within 24 h at ambient temperature in gas-permeable bags. Large roots, leaves, worms and rocks were removed by hand. The fresh soil was then slurried in a 3:1 ratio of millilitres of deionized water (DIW) to grams of soil (oven-dry equivalent). Slurry aliquots, 110 g each, were divided into 240 ml jars. We also prepared blank jars containing 100 ml DIW. The slurries and blank jars were pre-incubated in the dark in an anaerobic glove box for six days to deplete pre-existing O_2 , NO_2^- and NO_3^- . Each experiment was entirely carried out in an anaerobic glove box (Coy Laboratory Products) equipped with palladium catalyst packs to remove O_2 and a gas analyser to monitor O_2 concentrations, which remained at 0 ppm throughout the experiments. The glove-box headspace composition was approximately 90% N_2 , 8% carbon dioxide (CO_2) and 2% hydrogen.

We carried out a series of three experiments. In the first experiment, we incubated soil with the following treatments to determine if Feammox occurs in soils and to identify the relative importance of the Feammox pathways: $^{15}\text{NH}_4^+$ addition; $^{15}\text{NH}_4^+$ and Fe(III) addition; $^{15}\text{NH}_4^+$, Fe(III) and C_2H_2 addition; and soil-free jars (blanks) containing DIW ($n = 8$ per treatment). We sampled the jar headspace gas after 24 h of incubation. In the second experiment, we determined the timescale at which Feammox occurs after the addition of $^{15}\text{NH}_4^+$ and Fe(III) ($n = 8$). We sampled headspace gas from the same jars at 1.5 h intervals up to 9 h after NH_4^+ and Fe(III) addition. We calculated $^{30}\text{N}_2$ production rates for each sample from the linear change in $^{30}\text{N}_2$ mole fraction between two given time points. In the third experiment, we measured Feammox rates in soil at higher pH (≥ 6) to determine the effect of pH on Feammox rates. We incubated soil slurries with the following three treatments: $^{15}\text{NH}_4^+$ addition, $^{15}\text{NH}_4^+$ and Fe(III) addition, and soil-free blank jars containing DIW ($n = 8$ per treatment). We sampled the jar headspace gas for determination of $^{30}\text{N}_2$ mole fraction at 6, 12 and 25 h of incubation. In each experiment we added $6 \mu\text{g N } ^{15}\text{NH}_4\text{Cl g}^{-1}$ and sufficient Fe(III) to drive Feammox to NO_2^- using a stoichiometric molar ratio of 6:1 Fe(III) to $^{15}\text{NH}_4^+$. The amount of $^{15}\text{NH}_4^+$ added was chosen to increase our ability to detect changes in $^{29}\text{N}_2$ and $^{30}\text{N}_2$ mole fractions while keeping the NH_4^+ pool size at a realistic level. Ammonium pools typically range from 1 to $15 \mu\text{g N g}^{-1}$ in this tropical forest and are not correlated with O_2 availability^{7,8,26}.

At each sampling time point, each jar was shaken vigorously to equilibrate the N_2 between dissolved and gas phases. Duplicate gas samples were taken with gas-tight 500 μl syringes equipped with zero-volume stopcocks and immediately

analysed for isotopic composition for $^{29}\text{N}_2$ and $^{30}\text{N}_2$ mole fraction. A detailed description of the $^{15}\text{N}_2$ gas analysis technique is given in the Supplementary Methods. A third gas sample (50 ml) was stored for analysis of N_2O concentration on a Shimadzu GC-14A equipped with an electron capture detector.

After the final gas sampling, the slurries were subsampled for pH measurement using a pH electrode (Denver Instruments) and then extracted in 2 M KCl for colourimetric analysis of NH_4^+ and NO_3^- using an autoanalyser (Lachat Quik Chem flow injection analyser, Lachat Instruments). The extracts were shaken with phosphate and filtered to remove Fe that could interfere with colourimetric NO_3^- analysis²⁷. In the third experiment, we also used a 0.5 N HCl extraction to determine acid-extractable Fe(II) concentration. Owing to the high Fe(II) concentrations in the extracts, we used a modified ferrozine method²⁵ to quantify Fe(II) concentrations on a Genesys 20 spectrophotometer (ThermoFisher). Iron reduction rates were calculated from the linear change in Fe(II) concentrations between sampling time points. All extractions were carried out in the anoxic glove box.

We calculated $^{15}\text{N-NH}_4^+$ oxidation rates from the difference in jar headspace $^{29}\text{N}_2$ or $^{30}\text{N}_2$ mole fractions between samples and soil-free blanks (where $^{29}\text{N}_2$ or $^{30}\text{N}_2$ mole fraction = moles of $^{29}\text{N}_2$ or $^{30}\text{N}_2$ divided by moles of total N_2). To determine $^{15}\text{N-NH}_4^+$ oxidation rates from $^{15}\text{N}_2$ production, we used the stoichiometry of the Feammox to N_2 pathway. We determined the proportion of Feammox directly to $^{30}\text{N}_2$ as the difference between Feammox to $^{30}\text{N}_2$ and Feammox to NO_2^- and/or NO_3^- . A detailed description of the methods is given in the Supplementary Information.

Received 2 February 2012; accepted 26 June 2012; published online 29 July 2012

References

- Dalsgaard, T. & Thamdrup, B. Factors controlling anaerobic ammonium oxidation with nitrite in marine sediments. *Appl. Environ. Microbiol.* **68**, 3802–3808 (2002).
- Kuypers, M. M. M. *et al.* Massive nitrogen loss from the Benguela upwelling system through anaerobic ammonium oxidation. *Proc. Natl Acad. Sci. USA* **102**, 6478–6483 (2005).
- Schubert, C. J. *et al.* Anaerobic ammonium oxidation in a tropical freshwater system (Lake Tanganyika). *Environ. Microbiol.* **8**, 1857–1863 (2006).
- Clement, J. C., Shrestha, J., Ehrenfeld, J. G. & Jaffe, P. R. Ammonium oxidation coupled to dissimilatory reduction of iron under anaerobic conditions in wetland soils. *Soil Biol. Biochem.* **37**, 2323–2328 (2005).
- Shrestha, J., Rich, J., Ehrenfeld, J. G. & Jaffe, P. Oxidation of ammonium to nitrite under iron-reducing conditions in wetland soils: Laboratory, field demonstrations, and push-pull rate determination. *Soil Sci.* **174**, 156–164 (2009).
- Sawayama, S. Possibility of anoxic ferric ammonium oxidation. *J. Biosci. Bioeng.* **101**, 70–72 (2006).
- Silver, W. L., Herman, D. J. & Firestone, M. K. Dissimilatory nitrate reduction to ammonium in upland tropical forest soils. *Ecology* **82**, 2410–2416 (2001).
- Templer, P., Silver, W. L., Pett-Ridge, J., DeAngelis, D. & Firestone, M. K. Plant and microbial controls on nitrogen retention and loss in a humid tropical forest. *Ecology* **89**, 3030–3040 (2008).
- Chestnut, T., Zarin, D., McDowell, W. & Keller, M. A nitrogen budget for late-successional hillslope tabonuco forest, Puerto Rico. *Biogeochemistry* **46**, 85–108 (1999).
- Vitousek, P. M. & Howarth, R. W. Nitrogen limitation on land and in the sea: How can it occur. *Biogeochemistry* **13**, 87–115 (1991).
- Penton, C., Devol, A. & Tiedje, J. Molecular evidence for the broad distribution of anaerobic ammonium-oxidizing bacteria in freshwater and marine sediments. *Appl. Environ. Microbiol.* **72**, 6829–6832 (2006).
- Humbert, S. *et al.* Molecular detection of anammox bacteria in terrestrial ecosystems: Distribution and diversity. *ISME J.* **4**, 450–454 (2010).
- Jetten, M. *et al.* Biochemistry and molecular biology of anammox bacteria. *Crit. Rev. Biochem. Mol. Biol.* **4**, 65–84 (2009).
- Luther, G. W., Sundby, B., Lewis, B. L., Brendel, P. J. & Silverberg, N. Interactions of manganese with the nitrogen cycle: Alternative pathways to dinitrogen. *Geochim. Cosmochim. Acta* **61**, 4043–4052 (1997).
- Davidson, E. A. *et al.* Processes regulating soil emissions of NO and N_2O in a seasonally dry tropical forest. *Ecology* **74**, 130–139 (1993).
- Dubinsky, E. A., Silver, W. L. & Firestone, M. K. Tropical forest soil microbial communities couple iron and carbon biogeochemistry. *Ecology* **91**, 2604–2612 (2010).
- Ettwig, K. F. *et al.* Nitrite-driven anaerobic methane oxidation by oxygenic bacteria. *Nature* **464**, 543–547 (2010).
- Yoshinari, T., Hynes, R. & Knowles, R. Acetylene inhibition of nitrous oxide reduction and measurement of denitrification and nitrogen fixation in soil. *Soil Biol. Biochem.* **9**, 177–183 (1977).
- Cornell, R. M. & Schwertmann, U. *The Iron Oxides: Structure, Properties, Reactions, Occurrences, and Uses* (Wiley, 2003).
- Liptzin, D., Silver, W. L. & Detto, M. Temporal dynamics in soil oxygen and greenhouse gases in two humid tropical forests. *Ecosystems* **14**, 171–182 (2011).
- Sextstone, A. J., Revsbech, N. P., Parkin, T. B. & Tiedje, J. M. Direct measurement of oxygen profiles and denitrification rates in soil aggregates. *Soil Sci. Soc. Am. J.* **49**, 645–651 (1985).
- Faulkner, S. P. & Faulkner, W. H. Redox processes and diagnostic wetland soil indicators in bottomland hardwood forests. *Soil Sci. Soc. Am. J.* **56**, 856–865 (1992).
- Silver, W. L., Lugo, A. E. & Keller, M. Soil oxygen availability and biogeochemistry along rainfall and topographic gradients in upland wet tropical forest soils. *Biogeochemistry* **44**, 301–328 (1999).
- Schuur, E. A. G. & Matson, P. A. Net primary productivity and nutrient cycling across a mesic to wet precipitation gradient in Hawaiian montane forest. *Oecologia* **128**, 431–442 (2001).
- Liptzin, D. & Silver, W. L. Effects of carbon addition on iron reduction and phosphorus availability in a humid tropical forest soil. *Soil Biol. Biochem.* **41**, 1696–1702 (2009).
- Pett-Ridge, J., Silver, W. L. & Firestone, M. K. Redox fluctuations frame microbial community impacts on N-cycling rates in a humid tropical forest soil. *Biogeochemistry* **81**, 95–110 (2006).
- Yang, W. H., Herman, D. J., Liptzin, D. & Silver, W. L. A new approach for removing iron interference from soil nitrate analysis. *Soil Biol. Biochem.* **46**, 123–128 (2012).

Acknowledgements

We appreciate discussions with M. K. Firestone and field and laboratory assistance from C. Torrens, A. C. McDowell, A. W. Thompson, T. Wood, M. Wong and M. Almaraz. We also thank R. Daly for allowing us to use to her anoxic gas station. This research was supported by grants DEB-0543558, DEB-0842385 and ATM-0628720 to W.L.S., DEB-0841993 to K.A.W., and DDIG 0808383 as well as a Graduate Research Fellowship to W.H.Y. from the US National Science Foundation. Additional support came from NSF grant DEB-0620910 to the Institute of Tropical Ecosystem Studies, University of Puerto Rico, and the International Institute of Tropical Forestry as part of the Long-Term Ecological Research Program in the Luquillo Experimental Forest. The International Institute of Tropical Forestry provided considerable infrastructural and technical support.

Author contributions

W.H.Y. and W.L.S. designed the experiments with assistance from K.A.W.; W.H.Y. carried out the experiments with assistance from W.L.S.; W.H.Y. processed the samples and data; W.H.Y. and W.L.S. analysed the data and wrote the manuscript; K.A.W. carried out the thermodynamic calculations and contributed to the text.

Additional information

Supplementary information is available in the online version of the paper. Reprints and permissions information is available online at www.nature.com/reprints. Correspondence and requests for materials should be addressed to W.H.Y.

Competing financial interests

The authors declare no competing financial interests.